

Frequency Shifts in the Hydrogen-Bonded OH Stretch in Halide–Water Clusters. The Importance of Charge Transfer

Ward H. Thompson[†] and James T. Hynes^{*,†,‡}

Contribution from the Department of Chemistry and Biochemistry, University of Colorado, Boulder, Colorado 80309-0215, and Département de Chimie, UMR 8640, Ecole Normale Supérieure, 24, rue Lhomond, 75231 Paris, France

Received August 23, 1999. Revised Manuscript Received April 17, 2000

Abstract: We investigate the nature of the hydrogen bonding in the gas-phase halide–water clusters ($X^- \cdots H_2O$), with special emphasis on how the hydrogen bonding affects the frequency of the hydrogen-bonded OH stretch. We present two models for describing the electronic structure of the hydrogen bond. The first model (non-charge-transfer, or non-CT) includes only electrostatic interactions between the halide ion and the water molecule. The second is a two-valence-bond (VB) state model in which the first VB state has the charge character $X^- \cdots H_2O$ and the second is a charge-transfer VB state with electronic structure $XH \cdots OH^-$. We find that the non-CT model is inadequate for describing the frequency shifts in the hydrogen-bonded OH stretch for the halide–water clusters as compared with both experimental and ab initio results. Further, analysis of the charge distributions of the clusters obtained from ab initio calculations indicates significant contribution of charge transfer in the electronic structure. This analysis also allows the distinction to be made between polarization and charge-transfer effects. The two-VB state model is used to provide an estimate of the charge-transfer contribution, which increases in the order $I < Br < Cl < F$, a result in contrast with the order one would predict solely on the basis of the electron affinities. The ordering is due to the more dominant effects of the homolytic bond dissociation energies in the HX series and the smaller $O \cdots X$ distances for the smaller ions.

I. Introduction

In this paper we address the fundamental nature of hydrogen bonding by examining the red-shift in the OH stretching frequency upon formation of the hydrogen bond in binary halide–water clusters. These frequency red-shifts are a sensitive probe of the nature of hydrogen bonding since they are naturally related to the underlying electronic structure of the hydrogen bonds. In fact, the changes in the OH stretching frequency and absorption intensity have been previously studied in other systems by using a variety of approaches to gain insight into the charge-transfer contributions to hydrogen bonding;^{1–7} as is discussed in more detail within, it seems fair to say that this charge-transfer perspective—involving electron flow between the hydrogen-bonded partners—has not been the majority view. Here, we analyze the electronic structure of the four halide–water clusters, with particular emphasis on the hydrogen-bonded OH stretching frequency, to elucidate the role of charge-transfer effects. That these clusters could be especially revealing in this connection is suggested by the fact that Reed et al.⁸ have argued

via energy considerations that charge-transfer interactions constitute an important part of the binding energy for the fluoride– and chloride–water clusters.

The frequency shifts upon hydrogen bonding have also often been analyzed in terms of their relationship to the hydrogen bond energy.⁹ Some of the earliest work was carried out by Badger and co-workers,^{10,11} who measured the frequency shifts, $\Delta\omega$, in both the fundamental and the third harmonic for different compounds in pure liquids and binary mixtures. By combining their data with those of others, they found a direct relationship between the relative frequency shift, $\Delta\omega/\omega$, and the hydrogen bond strength. These authors found the relationship to be roughly linear but with a caveat: “...it is evident that there will be no very simple general relationship, but even if an approximate proportionality exists, as seems to be the case, it should be very useful.”¹⁰ Pimentel and co-workers⁹ measured $\Delta\omega$ for hydrogen-bonded complexes of a proton donor with a series of bases. They also found a direct relationship between the frequency shift and the enthalpy of formation for the hydrogen bond.⁹ These results displayed a distinct nonlinear relationship and, as anticipated by Badger and co-workers,^{10,11} one that was not universal for different systems.

More recently, Johnson and co-workers^{12,13} and Okumura and co-workers¹⁴ have experimentally measured the frequency shifts in the hydrogen-bonded OH stretch in the gas-phase binary halide–water clusters (with the exception of $F^- \cdots H_2O$),¹⁵

[†] University of Colorado.

[‡] Ecole Normale Supérieure.

(1) Tsubomura, H. *J. Chem. Phys.* **1955**, *23*, 2130–2133. Tsubomura, H. *J. Chem. Phys.* **1956**, *24*, 927–931.

(2) Nagakura, S.; Gouterman, M. *J. Chem. Phys.* **1957**, *26*, 881–886.

(3) Puranik, P. G.; Kumar, V. *Proc. Indian Acad. Sci.* **1963**, *A58*, 29–37. Puranik, P. G.; Kumar, V. *Proc. Indian Acad. Sci.* **1963**, *A58*, 327–335.

(4) Yoshida, Z.; Osawa, E. *J. Am. Chem. Soc.* **1965**, *87*, 1467–1469.

(5) Basila, M. R.; Saier, E. L.; Cousins, L. R. *J. Am. Chem. Soc.* **1965**, *87*, 1665–1669.

(6) Szczepaniak, K.; Tramer, A. *J. Phys. Chem.* **1967**, *71*, 3035–3039.

(7) Zilles, B. A.; Person, W. B. *J. Chem. Phys.* **1983**, *79*, 65–77.

(8) Reed, A. E.; Curtiss, L. A.; Weinhold, F. *Chem. Rev.* **1988**, *88*, 899–926.

Reed, A. E.; Weinhold, F. *J. Chem. Phys.* **1983**, *78*, 4066–4073. Reed, A. E.; Weinstock, R. B.; Weinhold, F. *J. Chem. Phys.* **1985**, *83*, 735–746.

(9) A brief review of work in this area up to ca. 1960 can be found in the following: Pimentel, G. C.; McClellan, A. L. *The Hydrogen Bond*; W. H. Freeman and Co.: San Francisco, 1960; pp 82–85.

(10) Badger, R. M.; Bauer, S. H. *J. Chem. Phys.* **1937**, *5*, 839–851.

(11) Badger, R. M. *J. Chem. Phys.* **1940**, *8*, 288–289.

(12) Ayotte, P.; Weddle, G. H.; Kim, J.; Johnson, M. A. *J. Am. Chem. Soc.* **1998**, *120*, 12361–12362.

indicating a nonlinear relationship between $\Delta\omega$ and the binding enthalpy, ΔH_{bind} ,¹⁶ as discussed below, this is strengthened if the theoretical result of Yates et al.¹⁷ for $\text{F}^- \cdots \text{H}_2\text{O}$ is included as well. But most importantly for our present purposes, these detailed measurements on halide–water clusters provide an excellent opportunity to investigate the nature of the hydrogen bond, particularly the charge-transfer contribution and its influence on $\Delta\omega$.

Certainly, numerous ab initio electronic structure calculations have been carried out on the halide–water clusters determining the energetics, equilibrium geometries, and vibrational frequencies.^{8,14,17–25} Here we concentrate not only on understanding the connection between the frequency shift and the binding energy of the halide–water clusters but also on elucidating the nature of the underlying electronic structure involved in the hydrogen bonding in these clusters. Specifically, we investigate the possible merits of a completely electrostatic model versus one that involves charge transfer from the anion to the water molecule. In valence bond (VB) language, the former involves the VB electronic structure $\text{X}^- \cdots \text{H}_2\text{O}$, while the latter involves in addition the VB state of electronic character $\text{XH} \cdots \text{OH}^-$. We examine the implications that these two pictures have for the frequency shifts in the halide–water clusters. It will be seen that charge-transfer effects are present and have a significant impact on $\Delta\omega$, though it is important to emphasize that they

do not alter the qualitative (i.e., linear or nonlinear) dependence of $\Delta\omega$ on ΔH_{bind} .

The nature of the hydrogen bond as fundamentally electrostatic^{26–30} or involving charge-transfer character^{8,9,31–34} has been debated for many years, continuing to the present time.³⁵ Of particular note in recent years are the energy decomposition scheme of Morokuma and co-workers^{27,28} and the work by Weinhold and collaborators⁸ in a similar vein. Both groups have developed approaches for decomposing the energy into contributions due to, e.g., electrostatics, exchange, polarization, and charge transfer. Morokuma and his group used their method to analyze hydrogen bonding in binary clusters; for example, for the water dimer they found that the charge-transfer contribution to the interaction energy was $\sim 20\%$ compared to $\sim 70\%$ electrostatic.²⁷ This analysis has led many to conclude that the question was resolved in favor of an electrostatic description. However, Weinhold and co-workers found charge transfer to be the dominant contribution to the binding energy in the water dimer by using their natural bond orbital analysis. In fact, in an examination of the fluoride– and chloride–water clusters, Reed et al.⁸ found the charge-transfer component to represent a large part of the binding energy. The reason for the differences between the two approaches is, naturally, the way that the electrostatic and charge-transfer contributions are defined in the two schemes. Specifically, the Morokuma approach counts as electrostatic contributions that in the Weinhold approach are counted as charge transfer.⁸ Thus, the Weinhold approach gives a consistently larger charge-transfer contribution to the energy than that of Morokuma.

We are further motivated in this work by the Mulliken picture of proton transfer of the hydrogen species.³⁴ (Reference 36 contains an extensive reference list connected with the Mulliken picture for both hydrogen bond complexes and proton-transfer systems.) In this perspective, the “proton” transfer is viewed as a coupled electron–hydrogen atom transfer. Due to the strong electronic coupling between the two VB states involved ($\text{AH} \cdots \text{B}$ and $\text{A}^- \cdots \text{HB}^+$), the transfer is not sequential but rather is concerted; nonetheless, it has a signature that the H species will have nearly constant charge that is significantly smaller than that of a fully charged proton.³⁶ It should be evident that this view of proton transfer reactions is intimately related to the charge-transfer view of hydrogen bonding (and its impact on stretching frequencies). The two share the same key element of electron transfer from the base lone pair to the antibonding orbital of the A–H (here, O–H) bond. In the case of proton

(13) Ayotte, P.; Weddle, G. H.; Kim, J.; Kelley, J.; Johnson, M. A. *J. Phys. Chem. A* **1999**, *103*, 443–447. Johnson, M. A. *J. Phys. Chem. A* **1998**, *102*, 3067–3071. Bailey, C. G.; Kim, J.; Dessent, C. E. H.; Johnson, M. A. *Chem. Phys. Lett.* **1997**, *269*, 122–127. Serxner, D.; Dessent, C. E. H.; Johnson, M. A. *J. Chem. Phys.* **1996**, *105*, 7231–7234.

(14) Choi, J.-H.; Kuwata, K. T.; Cao, Y.-B.; Okumura, M. *J. Phys. Chem. A* **1998**, *102*, 503–507. Johnson, M. S.; Kuwata, K. T.; Wong, C.-K.; Okumura, M. *Chem. Phys. Lett.* **1996**, *260*, 551–557.

(15) After submission of the present paper, new work by Johnson and co-workers on the $\text{F}^- \cdots \text{H}_2\text{O}$ cluster appeared in the literature: Ayotte, P.; Kelley, J. A.; Nielsen, S. B.; Johnson, M. A. *Chem. Phys. Lett.* **2000**, *316*, 455–459. The spectrum they obtained for the $\text{F}^- \cdots \text{H}_2\text{O}$ cluster contains a band at $\sim 2930 \text{ cm}^{-1}$ that they assign to the $2 \leftarrow 0$ overtone of the hydrogen-bonded OH stretching mode. This assignment is based, at least in part, on the calculations by Yates et al.¹⁷ and is consistent with a large ($\sim 2000 \text{ cm}^{-1}$) shift in the fundamental.

(16) The binding enthalpies are known accurately for the chloride, bromide, and iodide clusters¹⁸ and somewhat less accurately for the fluoride–water cluster.¹⁹ One of the peer reviewers of this paper has informed us of a very recent measurement of the fluoride–water binding enthalpy [Weiss, P.; Kemper, P. R.; Bowers, M. T.; Xantheas, S. S. *J. Am. Chem. Soc.* **1999**, *121*, 3531–3532]. This new value is $26.2 \pm 0.8 \text{ kcal/mol}$, as compared to 23.3 kcal/mol ,¹⁹ which we have used here. This new value will not affect the conclusions of the paper but will slightly modify the quantitative results for the $\text{F}^- \cdots \text{H}_2\text{O}$ cluster. Specifically, the non-CT model Lennard-Jones parameters and consequently the frequency red-shift will be changed slightly (see Table 2). Also, the CT component of the wave function (cf. Figure 8) will be larger with the new value.

(17) Yates, B. F.; Schaefer, H. F.; Lee, T. J.; Rice, J. E. *J. Am. Chem. Soc.* **1988**, *110*, 6327–6332.

(18) Hiraoka, K.; Mizuse, S.; Yamabe, S. *J. Phys. Chem.* **1988**, *92*, 3943–3952.

(19) Arshadi, M.; Yamdagni, R.; Kebarle, P. *J. Phys. Chem.* **1970**, *74*, 1475–1482.

(20) Kistenmacher, H.; Popkie, H.; Clementi, E. *J. Chem. Phys.* **1973**, *58*, 5627–5638. Kistenmacher, H.; Popkie, H.; Clementi, E. *J. Chem. Phys.* **1973**, *59*, 5842–5848.

(21) Xantheas, S. S. *J. Phys. Chem.* **1996**, *100*, 9703–9713.

(22) Xantheas, S. S.; Dang, L. X. *J. Phys. Chem.* **1996**, *100*, 3989–3995. Xantheas, S. S.; Dunning, T. H., Jr. *J. Phys. Chem.* **1994**, *98*, 13489–13497.

(23) Baik, J.; Kim, J.; Majumdar, D.; Kim, K. S. *J. Chem. Phys.* **1999**, *110*, 9116–9127.

(24) Zhao, X. G.; Gonzalez-Lafont, A.; Truhlar, D. G.; Steckler, R. *J. Chem. Phys.* **1991**, *94*, 5544–5558.

(25) Combariza, J. E.; Kestner, N. R. *J. Phys. Chem.* **1994**, *98*, 3513–3517. Combariza, J. E.; Kestner, N. R.; Jortner, J. *J. Chem. Phys.* **1994**, *100*, 2851–2864.

(26) Pauling, L. *The Nature of the Chemical Bond*; Cornell University Press: Ithaca, NY, 1944.

(27) Umevama, H.; Morokuma, K. *J. Am. Chem. Soc.* **1977**, *99*, 1316–1332.

(28) Morokuma, K. *Acc. Chem. Res.* **1977**, *10*, 294–300. Kitaura, K.; Morokuma, K. *Int. J. Quantum Chem.* **1976**, *10*, 325–340.

(29) Dykstra, C. E. *Acc. Chem. Res.* **1988**, *21*, 355–361 and references therein.

(30) Singh, U. C.; Kollman, P. A. *J. Chem. Phys.* **1984**, *80*, 353–355.

(31) Lewis, G. N. *Valence and the Structure of Atoms and Molecules*; The Chemical Catalog Co.: New York, 1923.

(32) Bratož, S. *Adv. Quantum Chem.* **1967**, *3*, 209–237.

(33) Ratajczak, H. *J. Phys. Chem.* **1972**, *76*, 3000–3004. Ratajczak, H. *J. Phys. Chem.* **1972**, *76*, 3991–3992.

(34) Mulliken, R. S. *J. Phys. Chem.* **1952**, *56*, 801–822. Mulliken, R. S. *J. Chim. Phys.* **1964**, *61*, 20–36. Mulliken, R. S.; Person, W. B. *Molecular Complexes: A Lecture and Reprint Volume*; Wiley-Interscience: New York, 1969.

(35) Recently, the results of Compton scattering experiments on water ice have been reported [Isaacs, E. D.; Shukla, A.; Platzman, P. M.; Hamann, D. R.; Barbiellini, B.; Tulk, C. A. *Phys. Rev. Lett.* **1999**, *82*, 600–603] that, based on comparisons with electrostatic and full quantum mechanical theoretical descriptions, support a covalent picture of hydrogen bonding in ice.

(36) Juanós i Timoneda, J.; Hynes, J. T. *J. Phys. Chem.* **1991**, *95*, 10431–10442.

transfer reactions this promotes the hydrogen transfer, whereas in hydrogen bonding it decreases the bond strength and thereby lowers the stretching frequency. While the Mulliken view is not a widely accepted perspective for proton-transfer reactions, it is supported by a detailed study by Ando and Hynes.³⁷ They examined the acid ionization of HCl in water and found in extensive ab initio calculations that the charge on H as it is being transferred is $\sim +0.3$,³⁷ not nearly +1 as would be expected in the traditional view of proton transfer. These authors have also studied the ionization of HF in water and found that the same conclusion holds for that system as well.^{38,39} Further, the picture of the electronic flow from the base nonbonding orbital to the AH antibonding orbital is supported in detail.³⁹ The Mulliken picture has also been applied in detailed studies of phenol–amine and other proton-transfer systems.^{36,40,41}

The remainder of the paper is organized as follows. We first present a preliminary model for describing the energetics and hydrogen-bonded OH stretching frequency shifts in the four halide–water clusters ($X^- \cdots H_2O$) in section II. This (non-charge-transfer, or non-CT) model contains no accounting for charge transfer from the halide to the water molecule and as such is a single-valence-bond state description which includes electrostatic effects. In section III.A we analyze the charge distributions of the clusters obtained from ab initio calculations to elucidate the charge-transfer contribution. Following this, we present a second (CT) model for the halide–water clusters which adds an additional valence bond state with charge-transfer character in section III.B. Finally, we offer some concluding remarks in section IV.

II. Non-CT Empirical Model

We first present an empirical model which contains no charge-transfer character. In this model, the potential describing the cluster is a single-valence-bond (electronically diabatic) surface with fixed charge character of the nature $X^- \cdots H_2O$. While we anticipate that this model will prove to be insufficient, it serves to reveal the necessity for the incorporation of CT

effects. In addition, we present the results of ab initio calculations at the MP2/SBK++ level;⁴² these are employed both as a guide for constructing the model and in providing an assessment of its validity.⁴³

This model is loosely based on the OPLS potentials of Jorgensen and co-workers, in which the interactions consist of Coulombic and Lennard-Jones terms.⁴⁴ The charges are placed on each hydrogen, the halide, and slightly (0.15 Å) away from the oxygen on the bisector of the H–O–H angle. The Lennard-Jones interaction,

$$V_{LJ}(r) = 4\epsilon \left[\left(\frac{\sigma}{r} \right)^{12} - \left(\frac{\sigma}{r} \right)^6 \right] \quad (1)$$

is between the halide and the water molecule, as represented by a single site located on the oxygen atom. The OPLS potential is a rigid water model. We have thus extended it by adding a Morse potential,

$$V_M(r) = D[1 - e^{-\beta(r-r_{eq})}]^2 \quad (2)$$

to account for the O–H_a stretch (denoting by H_a the hydrogen involved in the hydrogen bond and by H_b the “free” hydrogen) and an exponentially repulsive potential,

$$V_{rep}(r) = A e^{-B(r-q)} \quad (3)$$

between the hydrogens and X[−].

The parameters for this model were determined in the following way. The charges were taken from the OPLS model⁴⁴ (which is the same for H₂O as in the TIP4P model⁴⁵). The OH Morse parameters were taken to reproduce the experimentally observed 0 → 1 vibrational transition frequency,⁴⁶ $\omega_{01} = 3690 \text{ cm}^{-1}$.¹² The choice of parameters for the repulsive H–X[−] potentials was guided by ab initio calculations at the MP2/SBK++ level.⁴² The form in eq 3 is purposely chosen so that it cannot account for any charge transfer from the halide to the hydrogen.^{47,48} Finally, the Lennard-Jones parameters were

(43) Since there is no biradical contribution to the ground state of these clusters, a single-determinant-based approach should be adequate.

(44) Chandrasekhar, J.; Spellmeyer, D. C.; Jorgensen, W. L. *J. Am. Chem. Soc.* **1984**, *106*, 903–910.

(45) Jorgensen, W. L.; Chandrasekhar, J.; Madura, J. D.; Impey, R. W.; Klein, M. L. *J. Chem. Phys.* **1983**, *79*, 926–935.

(46) The transition frequency $\omega_{01} = 3690 \text{ cm}^{-1}$ is the value of the free (non-hydrogen-bonded) OH stretch in the halide–water clusters.¹² However, this value is very close to the average frequency of the symmetric and antisymmetric stretching bands (3707 cm^{-1}) in the isolated water molecule.¹²

(47) Ab initio calculations yield repulsive potentials for the H⁺⋯X[−] interactions for the bromide and iodide. The interaction of H with Cl[−] shows evidence of charge transfer at short internuclear distances (and large interaction energies). The H⁺⋯F[−] potential actually has a deep well (>1 eV), with the equilibrium structure characterized by a distribution of the excess negative charge over the entire molecule; (HF)[−] is stable with respect to dissociation to H and F[−] but not with respect to losing the excess electron to form HF (see, for example: Piecuch, P. *J. Mol. Struct.* **1997**, *437*, 503–536). The repulsive potentials in the non-CT model were obtained by fitting to the repulsive walls determined in ab initio calculations, where we have ignored the above-mentioned charge-transfer features for (HF)[−] and H⁺⋯Cl[−].

(48) It is important to note that, while it is not immediately obvious from the Born–Mayer potential parameters in Table 1, the repulsive H_a⋯X[−] potentials do, in fact, track the size of the anions. The parameter q is not meaningful without taking into consideration the parameters A and B in the Born–Mayer form (in fact, A and q are redundant; we take this form for convenience in fitting). The values of the Lennard-Jones parameters σ given in Table 1 map the anion size for all but fluoride. The σ value for fluoride is artificially large due to the combination of the nearness of F[−] to H₂O and the strong Coulomb forces imposed in the electrostatic model (recall that we have constrained the charges to be the same for all the clusters). Thus, the Lennard-Jones potential must be more repulsive (in this model) than one would expect on the basis of anion size. This is actually an initial indication of the shortcomings of the non-CT model for this cluster.

(37) Ando, K.; Hynes, J. T. *J. Phys. Chem. B* **1997**, *101*, 10464–10478.
Ando, K.; Hynes, J. T. *J. Mol. Liq.* **1995**, *64*, 25–37.

(38) Ando, K.; Hynes, J. T. *Discuss. Faraday Soc.* **1995**, *102*, 435–441.

(39) Ando, K.; Hynes, J. T. *J. Phys. Chem. A* **1999**, *103*, 10398–10408.

(40) Staib, A.; Borgis, D.; Hynes, J. T. *J. Chem. Phys.* **1995**, *102*, 2487–2505. Kim, H. J.; Staib, A.; Hynes, J. T. In *Femtochemistry and Femtobiology: Ultrafast Reaction Dynamics at Atomic-Scale Resolution*; Sundström, V., Ed.; Imperial College Press: London, 1997. Kiefer, P. M.; Hynes, J. T., to be submitted.

(41) Ando, K.; Hynes, J. T. *Adv. Chem. Phys.* **1999**, *110*, 381–430 and references therein.

(42) All ab initio calculations reported in this paper, with the exception of the natural bond orbital analysis, were carried out using the GAMESS package. Schmidt, M. W.; Baldridge, K. K.; Boatz, J. A.; Elbert, S. T.; Gordon, M. S.; Jensen, J. H.; Koseki, S.; Matsunaga, N.; Nguyen, K. A.; Su, S. J.; Windus, T. L.; Dupuis, M.; Montgomery, J. A. *J. Comput. Chem.* **1993**, *14*, 1347–1363. The natural bond orbital analysis (NBO Version 3.1, Glendening, E. D.; Reed, A. E.; Carpenter, J. E.; Weinhold, F.) was carried out using Gaussian 98, Revision A.6, (Frisch, M. J.; Trucks, G. W.; Schlegel, H. B.; Scuseria, G. E.; Robb, M. A.; Cheeseman, J. R.; Zakrzewski, V. G.; Montgomery, J. A., Jr.; Stratmann, R. E.; Burant, J. C.; Dapprich, S.; Millam, J. M.; Daniels, A. D.; Kudin, K. N.; Strain, M. C.; Farkas, O.; Tomasi, J.; Barone, V.; Cossi, M.; Cammi, R.; Mennucci, B.; Pomelli, C.; Adamo, C.; Clifford, S.; Ochterski, J.; Petersson, G. A.; Ayala, P. Y.; Cui, Q.; Morokuma, K.; Malick, D. K.; Rabuck, A. D.; Raghavachari, K.; Foresman, J. B.; Cioslowski, J.; Ortiz, J. V.; Stefanov, B. B.; Liu, G.; Liashenko, A.; Piskorz, P.; Komaromi, I.; Gomperts, R.; Martin, R. L.; Fox, D. J.; Keith, T.; Al-Laham, M. A.; Peng, C. Y.; Nanayakkara, A.; Gonzalez, C.; Challacombe, M.; Gill, P. M. W.; Johnson, B.; Chen, W.; Wong, M. W.; Andres, J. L.; Gonzalez, C.; Head-Gordon, M.; Replogle, E. S.; Pople, J. A. *Gaussian 98*, Revision A.6; Gaussian, Inc.: Pittsburgh, PA, 1998).

Table 1. Parameters for the Non-CT ($\text{H}_2\text{O}\cdots\text{X}^-$) Valence Bond State Potential

parameter	$\text{H}_b\text{OH}_a\cdots\text{F}^-$	$\text{H}_b\text{OH}_a\cdots\text{Cl}^-$	$\text{H}_b\text{OH}_a\cdots\text{Br}^-$	$\text{H}_b\text{OH}_a\cdots\text{I}^-$
Charges				
$q(\text{H}_b)$	+0.52	+0.52	+0.52	+0.52
$q(\text{O})$	-1.04	-1.04	-1.04	-1.04
$q(\text{H}_a)$	+0.52	+0.52	+0.52	+0.52
$q(\text{X})$	-1.00	-1.00	-1.00	-1.00
OH_a Morse Potential ^a				
D (eV)	5.1136	5.1136	5.1136	5.1136
β (\AA^{-1})	2.268	2.268	2.268	2.268
r_e (\AA)	0.9572	0.9572	0.9572	0.9572
$\text{X}^-\cdots\text{H}$ Interaction ^b				
A (eV)	0.4241	1.7578	8.4355	10.884
B (\AA^{-1})	5.6692	2.4921	2.6834	2.5511
q (\AA)	1.1642	1.1417	0.7673	0.8096
$\text{X}^-\cdots\text{O}$ Lennard-Jones Potential ^c				
ϵ (kcal/mol)	0.01543	1.0323	1.1407	1.9262
σ (\AA)	4.1254	3.6992	4.3416	4.5614

^a See eq 2. ^b See eq 3. ^c See eq 1.

Table 2. Experimental and Theoretical Binding Enthalpies/Energies and Absolute Values of the Hydrogen-Bonded OH Stretching Mode^a

cluster	binding enthalpy (kcal/mol)		frequency (cm^{-1})		
	expt	non-CT	expt	non-CT	ab initio
$\text{F}^-\cdots\text{H}_2\text{O}$	-23.3 ^b	-24.9		2688.4	2021.5
$\text{Cl}^-\cdots\text{H}_2\text{O}$	-14.7 ^c	-14.5	3130 ^d	3352.5	3106.1
$\text{Br}^-\cdots\text{H}_2\text{O}$	-11.7 ^c	-11.9	3270 ^d	3447.2	3234.9
$\text{I}^-\cdots\text{H}_2\text{O}$	-10.3 ^c	-10.4	3385 ^d	3510.8	3311.0
free OH stretch			3690 ^d	3692.6	3699.6

^a Experimental binding enthalpies and binding energies from the non-CT model are given (see ref 49). The frequencies for the free OH stretching mode are included for comparison. ^b Reference 19. ^c Reference 18. ^d Reference 12.

chosen as those that optimize the binding energies and geometries for the clusters to reproduce the experimental binding energies and ab initio geometries as well as possible. This optimization was carried out using a simulated annealing procedure to obtain the parameters. The model parameters are given in Table 1. This model potential reproduces well the experimental binding enthalpies^{18,19} of the four halide–water clusters, as can be seen from Table 2. With respect to the geometries, the $\text{O}-\text{X}^-$ equilibrium distance in the model potential is within 0.11 \AA of the ab initio result (at the MP2/SBK++ level), and $r_{\text{eq}}(\text{O}-\text{H}_a)$ within the model is within 0.06 \AA for the fluoride cluster and 0.04 \AA for the other three. Finally, the $\text{O}-\text{H}_a-\text{X}^-$ angles are within 4°, 6°, 9°, and 13° of the ab initio values for the F^- , Cl^- , Br^- , and I^- clusters, respectively.

Since we are interested in the physical nature of the hydrogen bonding, we consider a simplified description of the vibrations of the complex. Specifically, we concentrate on an approximate one-dimensional description accounting only for the hydrogen-bonded OH stretch. That is, in calculating frequencies, potential energy surfaces, charges, etc., all the atoms of the $\text{X}^-\cdots\text{H}_a\text{OH}_b$ cluster are frozen in position except for H_a . The $\text{H}_a-\text{O}-\text{H}_b$ angle is frozen at 104.52° and the OH_b distance at 0.9572 \AA . The position of X^- relative to the water molecule is frozen at its

(49) In general, the binding energy can differ significantly from the binding enthalpy. However, we have estimated that for these clusters, the difference is less than ~0.6 kcal/mol, which is consistent with calculations by Xantheas.²¹ This difference is not significantly greater than the uncertainty in the experimentally measured binding enthalpies.^{18,19} Thus, it is not unreasonable to use our calculated binding energies as a substitute for binding enthalpies for these systems.

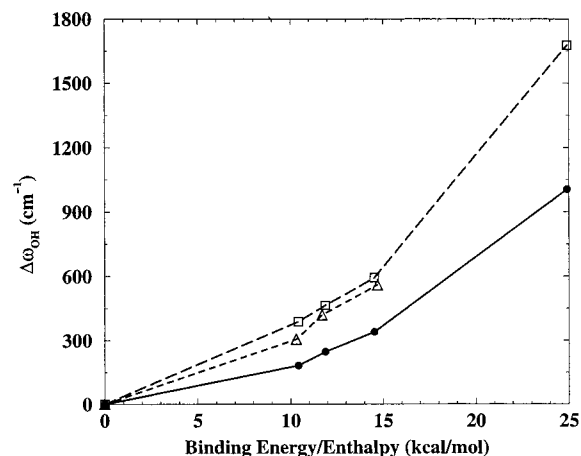


Figure 1. Frequency shifts in the water OH stretch upon hydrogen bonding with halides as a function of the complex binding energy. The experimental results of Ayotte et al.¹² (short dashed line with triangles) are compared with calculations using the non-CT model (solid line with circles) and ab initio calculations (long dashed line with squares). The experimental frequency shifts are plotted using the experimental binding enthalpies.¹⁸ Both calculated results are plotted using the binding energies obtained from the non-CT model.⁴⁹

equilibrium geometry, and the $\text{O}-\text{H}_a$ distance is increased along the direction of the bond (with a concomitant decrease in the H_a-X distance).

We now consider the frequency shifts predicted by the non-CT model and ab initio calculations and compare them to the experimental results of Johnson and co-workers.^{12,50} Figure 1 shows the frequency shift in the hydrogen-bonded OH stretch (the $\omega_1-\omega_0$ transition frequency) as a function of the cluster binding energy for the four halide–water clusters. The binding enthalpies and absolute values of the frequencies used in Figure 1 are given in Table 2. The calculated frequency shifts are obtained by generating a one-dimensional potential energy surface in the $r(\text{O}-\text{H}_a)$ coordinate as described in the preceding paragraph.⁵¹ The one-dimensional potential energy surfaces for both the non-CT model and from ab initio calculations were constructed using the same cluster geometries. Thus, in comparing those results, the differences are due only to the way in which the energy is calculated. This is a useful comparison as it eliminates factors due to the simplified description of the vibration and focuses directly on the electronic structure. The one-dimensional Schrödinger equation was solved for the OH vibrational energy eigenvalues and eigenstates using a sinc-function discrete variable representation basis.⁵²

While the experimental data do not allow an unambiguous assignment of the relationship between $\Delta\omega$ and the binding

(50) Note that the experimental frequencies reported by Ayotte et al.¹² have been adjusted to remove the effects due to a Fermi resonance between the hydrogen-bonded OH stretch and the overtone of the intramolecular bend.

(51) There are two primary issues associated with this approximate model of the vibrations in the clusters. First, the clusters can interconvert between the two possible hydrogen-bonded structures (i.e., the hydrogen atom which is hydrogen-bonded can be switched). This possibility has been discussed by Okumura and co-workers in ref 14. The facility with which this interconversion takes place is not fully understood (e.g., is it tunneling or “over the barrier” motion?) and will be different for the four halide–water clusters. Second, the intermode coupling to the other vibrations of the clusters is neglected and can affect the frequency red-shifts. Yates et al.¹⁷ found, using a perturbation theory analysis, that this intermode coupling has a much smaller contribution to the frequency shifts than the intramode anharmonicity (which is fully included in our model) for the $\text{F}^-\cdots\text{H}_2\text{O}$ cluster. It is important to note that the neglect of these two effects will not alter the fundamental conclusions presented in this paper regarding the role of charge transfer in the frequency shifts.

(52) Colbert, D. T.; Miller, W. H. *J. Chem. Phys.* **1992**, *96*, 1982–1991.

enthalpy as linear or nonlinear, both the non-CT model and ab initio calculations show a distinct nonlinear dependence. Thus, we note that a nonlinear relationship between $\Delta\omega$ and ΔH_{bind} results from a purely electrostatic model as well as from a more complete description incorporating polarization and charge-transfer effects. This is made particularly clear by the inclusion of the results for the $\text{F}^- \cdots \text{H}_2\text{O}$ cluster, for which experimental frequency shifts are not available. These results are consistent with those of Yates et al.,¹⁷ who previously found a value of 1853 cm^{-1} (including intermode coupling) for the hydrogen-bonded OH stretching frequency in $\text{F}^- \cdots \text{H}_2\text{O}$. Combination of this 1988 theoretical result¹⁷ with the more recent experiments^{12–14} clearly supports a nonlinear relationship between $\Delta\omega$ and ΔH_{bind} . This value compares with the present result of 2021.5 cm^{-1} (see Table 2). Thus, it seems clear that measurements on the $\text{F}^- \cdots \text{H}_2\text{O}$ cluster could lead to a clearer understanding of the relationship between the frequency shifts and the charge-transfer character in these systems.^{15,53}

The non-CT model yields frequency shifts that are significantly lower than both the experimental and ab initio results. The ab initio frequency shifts, while consistently higher, are in good agreement with the experimental values for the iodide, bromide, and chloride clusters. As mentioned above, the non-CT model and ab initio results both indicate a nonlinear relationship between $\Delta\omega$ and binding energy, with the ab initio calculations predicting much larger red-shifts. In addition, the discrepancy between the two calculations increases with the binding energy (i.e., going from iodide to fluoride).

An interesting side point concerns whether the frequency shift for a cluster originates from a change in the harmonic force constant⁵⁴ or an increase in the bond anharmonicity.⁵⁵ In agreement with the results of Yates et al.¹⁷ for the fluoride–water cluster, we find in the ab initio calculations that changes in the harmonic force constants and the bond anharmonicities both contribute to the observed frequency shift. Thus, both of these effects are important and must be included in a description of these clusters.

Our goal in this section was to develop a consistent electrostatic model for the set of halide–water clusters in which the charges are based on a widely used potential for (rigid) water. We do not mean to assert that a purely electrostatic model could not correctly reproduce the red-shifts in the hydrogen-bonded OH stretching frequency. For example, with a priori knowledge of the frequency shifts one could, in principle, construct a non-CT model which gives the correct binding energies and frequencies by adjusting the parameters to do just that. It is in this sense that care must be taken in drawing conclusions. The development of an electrostatic model that reproduces such data is not proof that the actual system is purely electrostatic in nature but is rather a reflection of the flexibility in fitting the model.

However, the failure of the non-CT model to correctly predict the frequency shifts while yielding excellent binding energies and reasonable geometries is indicative of the presence of charge transfer. One might instead argue that the differences between the non-CT model presented here and the ab initio results are due to polarization and not to charge transfer. This issue is

(53) It may seem that the $\text{F}^- \cdots \text{H}_2\text{O}$ cluster, with its much larger frequency shift, is a special case and should not be grouped with the other halide–water clusters. However, the $\text{F}^- \cdots \text{H}_2\text{O}$ cluster is qualitatively the same as the other halide–water clusters, with the only differences occurring in the quantitative features, e.g., in the amount of charge-transfer character, as seen in the present results.

(54) Reimers, J. R.; Watts, R. O. *Chem. Phys.* **1984**, *85*, 83–112.

(55) Sceats, M. G.; Rice, S. A. *J. Chem. Phys.* **1979**, *71*, 973–982.

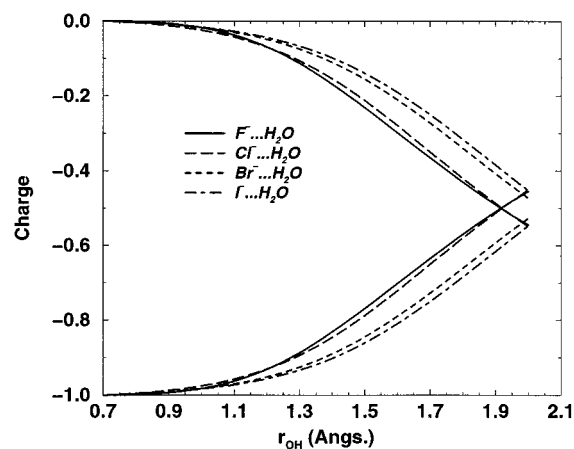


Figure 2. Changes in the Löwdin charges for the H_2O and X^- fragments in the $\text{H}_b\text{OH}_a \cdots \text{X}^-$ gas-phase clusters as a function of the $\text{O}-\text{H}_a$ distance, resulting from the ab initio calculations. The curves increasing as a function of $r(\text{O}-\text{H}_a)$ represent the charge on X^- , while those decreasing represent the charge on H_2O . The curves have been shifted so that the charges on H_2O and X^- for $r(\text{O}-\text{H}) = 0.7 \text{ \AA}$ are 0 and -1 , respectively.

addressed next, along with more direct estimates of the charge-transfer contributions in these clusters.

III. Inclusion of Charge Transfer

A. Analysis of Charge Distributions. In addition to the obvious shortcomings of the non-CT model, there is further evidence pointing to the importance of charge transfer in halide–water clusters. In particular, ab initio calculations can be used to obtain an estimate of the charge on each atom. It is instructive to look at these charges as a function of the $\text{O}-\text{H}$ distance. In Figure 2, the changes in the total charges on the H_2O moiety and the halide (as determined from ab initio calculations at the MP2/SBK++ level) are plotted for the four different clusters as a function of $r(\text{O}-\text{H}_a)$. Note that this allows us to distinguish between the effects of polarization, where the charge within the water molecule is redistributed but the total charge remains constant, and charge transfer, where charge is exchanged between the water molecule and the halide. For small $r(\text{O}-\text{H}_a)$ distances ($\sim 0.7\text{--}1.0 \text{ \AA}$), only small changes in the total H_2O and X^- charges are observed. This indicates that polarization effects dominate charge transfer in this region (vide infra). However, it is clear from Figure 2 that significant charge transfer is occurring at large $\text{O}-\text{H}$ separations as H approaches X^- , and in fact this is a large effect with ~ 0.5 unit charge transferred from X^- to H_2O at the largest bond distances. Note that the F^- and Cl^- clusters exhibit larger charge-transfer effects. While the precise order is less clear at smaller $r(\text{O}-\text{H}_a)$, it appears that, for the most part, the charge transfer increases in the order $\text{I} < \text{Br} < \text{Cl} < \text{F}$.

Additional information can be gained by examining the charges on the H_aX and OH_b fragments (the configuration of the charge-transfer state has charges of 0 and -1 for these fragments). The dependence of the Löwdin charges of H_aX and OH_b on $r(\text{O}-\text{H}_a)$ is shown in Figure 3 for the four halide–water clusters. At very small $r(\text{O}-\text{H}_a)$ these charges take on values of ~ -0.3 and -0.7 for OH_b and H_aX , respectively, reflecting the non-CT character of the clusters as seen in Figure 2. However, as the $\text{O}-\text{H}_a$ bond is stretched, with a corresponding reduction in the H_a-X distance, the charges change rapidly and approach the -1 and 0 values expected for the charge-transfer state at large $r(\text{O}-\text{H}_a)$. Here, the differences in the role

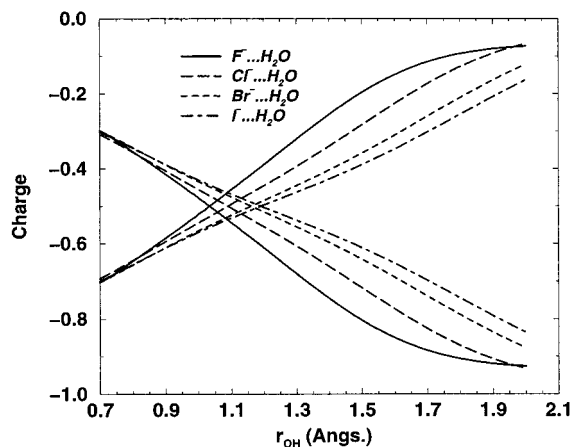


Figure 3. Löwdin charges for the H_aX and OH_b fragments in the $H_bOH_a\cdots X^-$ gas-phase clusters as a function of the $O-H_a$ distance. The curves increasing as a function of $r(O-H_a)$ represent the charge on H_aX , while those decreasing represent the charge on OH_b . (Note that the curves in this figure have not been shifted as those in Figure 2 were.)

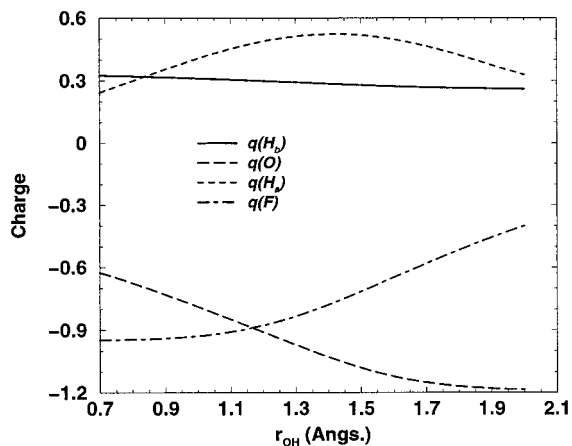


Figure 4. Löwdin atomic charges for the $H_bOH_a\cdots F^-$ gas-phase clusters as a function of the $O-H_a$ distance.

of charge transfer in the four clusters are more apparent. Again, the charge-transfer character for a given $r(O-H_a)$ increases in the order $I < Br < Cl < F$.

It is also instructive to examine the charges on the individual atoms. These are shown in Figure 4 versus $r(O-H_a)$ for the $F^-\cdots H_2O$ cluster. There are several noteworthy features. First, it is clear that the free hydrogen (H_b) is very much a spectator and does not play a significant role (by accepting or donating charge) in either polarization of the water molecule or charge transfer. Second, it can be seen that at smaller $O-H_a$ distances, polarization is important. As $r(O-H_a)$ is lengthened from 0.7 Å, the bond becomes increasingly polarized by the F^- , with the hydrogen (H_a) gaining positive charge and the oxygen gaining negative charge. It is important to note that the charge on the fluoride is relatively constant in this region. However, for larger $O-H_a$ separations, charge transfer is dominant, as seen from the large decrease in the negative charge on the fluoride (from ~ -0.95 to ~ -0.40). At the same time, the charge on the oxygen becomes more negative (from ~ -0.57 to ~ -1.18). Meanwhile, the charge on the hydrogen (H_a) changes little in comparison, indicating that the charge transfer is really taking place from F^- to O through (but not to) H_a . The other halide–water clusters show qualitatively similar behavior, with the primary differences located in the quantitative features of the “turn-on” of charge transfer.

Table 3. Natural Bond Orbital (NBO) Occupations for the $O-H_a$ Bonding, $O-H_a^*$ Antibonding, and Halide Lone Pair (lp) Orbitals as a Function of $r(O-H_a)$, Along with the Natural Population on H_a

orbital	$r(O-H_a)$ (Å)				
	0.9	1.0	1.1	1.2	1.3
$H_bOH_a\cdots F^-$					
$O-H_a$	1.9997	1.9994	1.9991	1.9987	1.9982
$O-H_a^*$	0.0263	0.0489	0.0790	0.1152	0.1548
$F^-(lp)$	1.9709	1.9477	1.9178	1.8825	1.8439
H_a	0.4781	0.4458	0.4315	0.4261	0.4213
$H_bOH_a\cdots Cl^-$					
$O-H_a$	1.9998	1.9996	1.9993	1.9990	1.9987
$O-H_a^*$	0.0158	0.0323	0.0572	0.0916	0.1360
$Cl^-(lp)$	1.9817	1.9644	1.9388	1.9041	1.8600
H_a	0.5020	0.4753	0.4702	0.4810	0.5011
$H_bOH_a\cdots Br^-$					
$O-H_a$	1.9998	1.9996	1.9994	1.9991	1.9988
$O-H_a^*$	0.0078	0.0167	0.0312	0.0528	0.0829
$Br^-(lp)$	1.9906	1.9811	1.9661	1.9440	1.9136
H_a	0.5066	0.4772	0.4674	0.4726	0.4880
$H_bOH_a\cdots I^-$					
$O-H_a$	1.9998	1.9996	1.9993	1.9990	1.9988
$O-H_a^*$	0.0058	0.0128	0.0246	0.0426	0.0685
$I^-(lp)$	1.9928	1.9853	1.9730	1.9546	1.9284
H_a	0.5124	0.4839	0.4744	0.4796	0.4953

Finally, we present the results of a natural bond orbital (NBO) analysis⁸ of the four halide–water clusters. This is particularly useful in connection with the Mulliken picture, as it gives the occupations of the $O-H_a$ bonding and antibonding orbitals and the lone pair orbitals on the halide. The occupations for these three orbitals as well as the natural population on H_a are given in Table 3 for several values of the $r(O-H_a)$ coordinate. In all cases, the occupation of the $O-H_a$ bonding remains essentially constant as $r(O-H_a)$ is increased. The natural population on the hydrogen-bonded H_a also changes little (by less than 0.05) over the range of $r(O-H_a)$ shown. The key point, however, is that the occupation of the $O-H_a$ antibonding orbital increases in concert with the decrease of the lone pair on the halide as the $O-H_a$ bond is stretched. This is precisely what would be expected on the basis of the Mulliken picture: as the bond is stretched, electron density is transferred from the halide lone pair orbital to the $O-H_a$ antibonding orbital, while the charge on H_a remains relatively constant. At all values of $r(O-H_a)$, the magnitude of the charge transfer from the halide lone pair to the $O-H_a$ antibonding orbital increases in the order $I < Br < Cl < F$; this is consistent with the analysis of the Löwdin charges above.

B. Two-VB State Model Including Charge Transfer. It is important to verify that the clusters can really be described by including a charge-transfer state. To this end, we extend the non-CT model by adding a second valence bond state, representing the $HO^-\cdots HX$ configuration. The goal here is twofold: first, to show that this is a consistent representation of the electronic structure of the clusters, and second, to further investigate the role of charge transfer in the frequency shifts of the hydrogen-bonded OH stretch.

In this two-VB state description, the neutral (i.e., the non-CT) state is taken to be the ab initio surface for the $I^-\cdots H_2O$ cluster. It is important to stress that we are thereby taking a conservative approach in estimating the role of charge transfer by implicitly assuming in this analysis that there is no charge-transfer contribution for the iodide cluster. The reason for choosing a different neutral VB state than that used in section II is that the non-CT model of that section was constructed to provide a *complete* description of the clusters. Thus, it is not

Table 4. Parameters for the Charge-Transfer ($\text{HO}^- \cdots \text{HX}$) Valence Bond State Potential

parameter	$\text{H}_b\text{O}^- \cdots \text{H}_a\text{F}$	$\text{H}_b\text{O}^- \cdots \text{H}_a\text{Cl}$	$\text{H}_b\text{O}^- \cdots \text{H}_a\text{Br}$
Charges			
$q(\text{H}_b)$	+0.35	+0.35	+0.35
$q(\text{O})$	-1.35	-1.35	-1.35
$q(\text{H}_a)$	+0.30	+0.18	+0.12
$q(\text{X})$	-0.30	-0.18	-0.12
H_aX Morse Potential ^a			
D (eV)	5.87	4.430	3.75
β (\AA^{-1})	2.3253	1.933	1.862
r_c (\AA)	0.9171	1.2746	1.413
$\text{H}_b\text{O}^- \cdots \text{H}_a$ Interaction ^b			
A (eV)	0.8299	0.8299	0.8299
B (\AA^{-1})	8.5	8.5	8.5
q (\AA)	0.94	0.94	0.94
Energy Shift ^c			
ΔE (eV)	0.8136	2.4716	2.8996

^a See eq 2. ^b See eq 3. ^c See eq 4.

an accurate depiction of the neutral VB state in a two-state model for these systems.

The potential surface for the $\text{I}^- \cdots \text{H}_2\text{O}$ cluster as a function of $r(\text{O}-\text{H}_a)$ is represented as an eighth-order polynomial obtained by a least-squares fit to the ab initio data.⁵⁶ The minimum in the $\text{I}^- \cdots \text{H}_2\text{O}$ one-dimensional surface is taken to be -10.3 kcal/mol (where the zero of energy is fully separated I^- and H_2O). This is the experimental binding enthalpy of the cluster.¹⁸ In turn, the minima in the electronically adiabatic ground-state surfaces obtained from ab initio calculations for the other clusters are taken from their respective experimental binding enthalpies (see Table 2).

The diabatic potential for the CT state is generated along the same lines as that for the non-CT state in section II. Specifically, charges are placed on each atom which are roughly consistent with the dipole moments of OH^- and the HX molecules.⁵⁷ A Morse potential, eq 2, is used to describe the covalent HX bond, while a purely repulsive exponential potential, eq 3, in $r(\text{O}-\text{H}_a)$ is used for the $\text{H} \cdots \text{OH}^-$ interaction based on ab initio calculations at the MP2/SBK++ level. (For the fluoride-water cluster, an additional repulsive term of the form $(\sigma_{\text{HF}}/r_{\text{HF}})^{12}$, with $\sigma_{\text{HF}} = 0.529 \text{ \AA}$, is added in the H_a-F coordinate to compensate for the fact that the Morse potential repulsion is too "soft".) Finally, the Lennard-Jones interaction between X and O used in the non-CT potential is included. Naturally, there is an energy shift of this surface relative to the non-CT surface consistent with choosing the zero of energy as the fully separated X^- and H_2O configuration. This energy shift is given by appropriate differences in the bond dissociation energies and electron affinities:

$$\Delta E = D(\text{H}-\text{OH}) - D(\text{H}-\text{X}) + \text{EA}(\text{X}) - \text{EA}(\text{OH}) \quad (4)$$

The parameters used for the CT states are listed in Table 4.

The valence bond and adiabatic ground-state surfaces (including the electronic coupling) for the $\text{F}^- \cdots \text{H}_2\text{O}$ cluster are plotted as a function of $r(\text{O}-\text{H}_a)$ in Figure 5. The procedure for generating the electronic coupling at a given value of $r(\text{O}-\text{H}_a)$ is the following: (1) the neutral and CT valence bond state energies are calculated; (2) the electronically adiabatic ground-



Figure 5. Valence bond states for the $\text{H}_b\text{OH}_a \cdots \text{F}^-$ gas-phase clusters as a function of the $\text{O}-\text{H}_a$ distance. The neutral and CT states are shown along with the electronic coupling (V_{coup}), the ab initio surface used to determine the coupling (V_{gr}), and the result of diagonalizing the VB states with the coupling (V_{diag}). (See the text for a discussion of the behavior at large $\text{O}-\text{H}_a$ distance.)

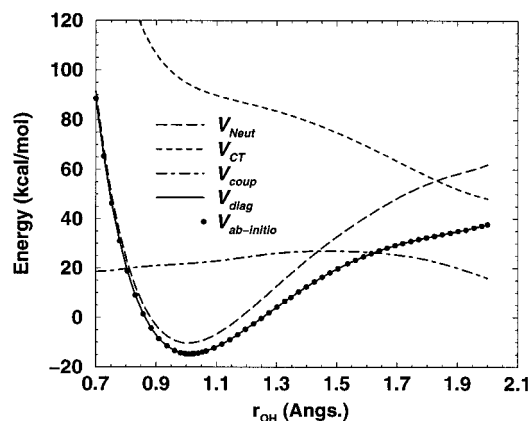


Figure 6. Same as Figure 5 but for the $\text{H}_b\text{OH}_a \cdots \text{Cl}^-$ gas-phase cluster.

state potential is obtained from an ab initio calculation at the MP2/SBK++ level; and (3) the electronic coupling is then computed through the knowledge of these three energies via the relation⁵⁸

$$V_{\text{coup}} = [(V_{\text{neut}} - V_{\text{gr}})(V_{\text{CT}} - V_{\text{gr}})]^{1/2} \quad (5)$$

As a check, the diabatic states are diagonalized using this coupling to reobtain the ground state. There is only a discrepancy in the $\text{F}^- \cdots \text{H}_2\text{O}$ case, specifically in the potential at large $r(\text{O}-\text{H}_a)$. This is due to the fact that the neutral state is lower in energy than the ab initio ground state here; the I^- - O distance is much larger than the F^- - O distance, and so the neutral state does not contain the correct X^- - H_a repulsive interaction for the other clusters. However, this is problematic only for large values of $r(\text{O}-\text{H}_a)$ (where H_a is close to F^-) and does not affect the present results. Note that the vibrational frequencies are determined by the potential at smaller values of $r(\text{O}-\text{H}_a)$; the outer classical turning point for the $\nu = 1$ state is $\sim 1.4 \text{ \AA}$.

The potential energy surfaces for the chloride- and bromide-water clusters are shown in Figures 6 and 7. Note that the energy of the V_{CT} state increases significantly on going down the halide group from F to Br . This can be attributed in large measure to the energy shift, ΔE (cf., eq 4 and Table 4), and more

(56) Press, W. H.; Flannery, B. P.; Teukolsky, S. A.; Vetterling, W. T. *Numerical Recipes, The Art of Scientific Computing*; Cambridge University Press: Cambridge, U.K., 1992.

(57) Herzberg, G. *Molecular Spectra and Molecular Structure I. Spectra of Diatomic Molecules*; Van Nostrand: New York, 1950. Huber, K. P.; Herzberg, G. *Molecular Spectra and Molecular Structure IV. Constants of Diatomic Molecules*; Van Nostrand: New York, 1979.

(58) It is assumed throughout that the two-valence-bond states (neutral and CT) are orthogonal; see the discussion in ref 36 and the following: Bianco, R.; Hynes, J. T. *J. Chem. Phys.* **1995**, *102*, 7864-7884.

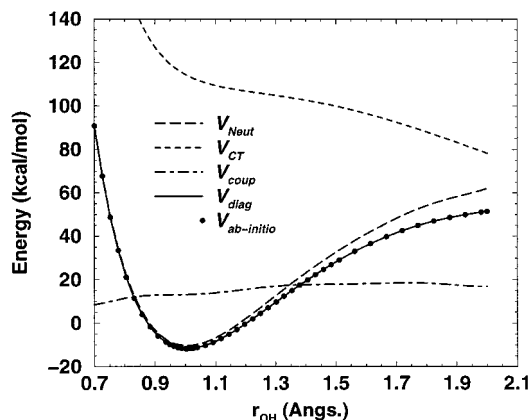


Figure 7. Same as Figure 5 but for the $H_bOH_a \cdots Br^-$ gas-phase cluster.

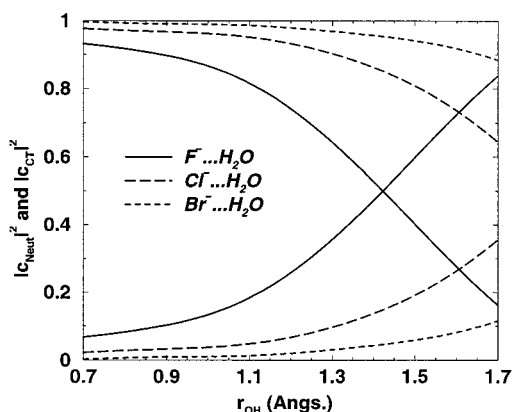


Figure 8. Composition of the adiabatic ground state in terms of the VB states as given by $|c_{\text{neut}}|^2$ and $|c_{\text{CT}}|^2$ as a function of the O–H_a distance.

specifically to the decreasing homolytic bond dissociation energy dominating the decreasing electron affinity as we move down the group (though the anomalously low electron affinity of F actually increases the effect).⁵⁹ We will return to this issue below.

The composition of the adiabatic ground state in terms of the neutral and CT valence bond states as a function of $r(\text{O}–\text{H}_a)$ is shown in Figure 8. Specifically, $|c_{\text{neut}}|^2$ and $|c_{\text{CT}}|^2$ are plotted, where c_{neut} and c_{CT} are the coefficients of the VB states in representing the ground state:

$$\Psi_g = c_{\text{neut}}\psi_{\text{neut}} + c_{\text{CT}}\psi_{\text{CT}} \quad (6)$$

It can immediately be seen that the charge-transfer character of the ground state ($|c_{\text{CT}}|^2$) increases as the OH_a bond is stretched, and consequently the H_aX distance is reduced (with the exception of very small $r(\text{O}–\text{H}_a)$ in the fluoride–water cluster). Note that in the region around $r(\text{O}–\text{H}_a) \sim 1.0$ Å, roughly the equilibrium distance, there is significant charge-transfer character in the fluoride–water cluster, a feature which decreases on going down the group of halides (from F to I). Recall that we have assumed that there is no charge transfer occurring in the iodide–water cluster, so these are relative results. That is, the results plotted in Figure 8 show the difference between the charge-transfer character of the $I^- \cdots H_2O$ cluster and that of the other three halide–water clusters. The ab initio calculations for the $I^- \cdots H_2O$ cluster necessarily include both polarization and charge-transfer contributions. Thus, these effects, to the degree

that they are evidenced in the iodide–water cluster, are implicitly accounted for in the neutral states of the other three clusters.

The classical outer (large $r(\text{O}–\text{H}_a)$) turning points for the one-dimensional O–H stretching potential in the $F^- \cdots H_2O$ are 1.2 and 1.4 Å for the $\nu = 0$ and $\nu = 1$ states, respectively. Even though some polarization and charge-transfer effects are included in the neutral VB state in the model (i.e., those present in the iodide–water cluster), at these distances the charge-transfer state coefficient $c_{\text{CT}} \approx 0.50$ and 0.69 , respectively. For the $Cl^- \cdots H_2O$ cluster, the values of the coefficient c_{CT} at the outer turning points are 0.23 and 0.28 for the $\nu = 0$ and $\nu = 1$ states, respectively. We note in passing that clearly the importance of charge transfer for the red-shifts in the OH stretching frequency will be greater for higher overtones since the higher vibrational states will have amplitude at larger values of $r(\text{O}–\text{H}_a)$; these deserve further study.⁶⁰

At a given value of $r(\text{O}–\text{H}_a)$, the charge-transfer character decreases as we move down the halide group (i.e., $F > Cl > Br > I$). This is an interesting result. On the basis of electron affinities⁵⁹ alone, the iodide–water cluster would be expected to have the largest charge-transfer contribution. However, a critical mitigating factor is the $X^- \cdots O$ distance in the four clusters. The smaller $F^- \cdots O$ equilibrium distance (2.63 Å) in the cluster significantly reduces the separation of charge penalty when charge transfer occurs in this cluster relative to the Cl^- , Br^- , and I^- clusters, which all have larger $X^- \cdots O$ distances (3.20, 3.53, and 3.75 Å, respectively). Note also that, as discussed above, the relative position in energy of the CT state for the F^- cluster is significantly lower than for the other halides, due in large part to the homolytic bond dissociation energy of HF, which is nearly 1.5 eV greater than that for HCl. This presents another connection with the Mulliken picture of proton transfer. For the HX series of acids, the homolytic bond dissociation energy is the primary factor in determining the relative acidities.^{26,39,61}

IV. Concluding Remarks

We have presented two models for the set of gas-phase halide–water binary clusters with the purpose of understanding the red-shifts in the hydrogen-bonded OH stretching frequency and elucidating the nature of the hydrogen bond. The first (non-CT) model is purely electrostatic in nature, while the second also includes contributions from charge transfer from the halide to the OH stretch antibonding orbital. A simplified one-dimensional model is used to describe the vibrations of the hydrogen-bonded OH stretching mode. The non-CT model yields significantly smaller red-shifts than those obtained from ab initio calculations or found in the experimental measurements.¹² The ab initio and experimental results are in good agreement. The second model includes two valence bond states, one with neutral (no charge transfer, i.e., H_2O and X^-) and the other with charge-transfer (HO^- and HX) character. By construction, this model gives red-shifts that are identical to the ab initio calculations.

(60) At some point, vibrational predissociation will complicate the analysis, but this is itself an interesting phenomenon (cf.: Staib, A.; Hynes, J. T. *Chem. Phys. Lett.* **1993**, *204*, 197–205. Heilweil, E. J. *Science* **1999**, *283*, 1467–1468. Woutersen, S.; Emmerichs, U.; Nienhuys, H.-K.; Bakker, H. J. *Phys. Rev. Lett.* **1998**, *81*, 1106–1109. Nienhuys, H.-K.; Woutersen, S.; van Santen, R. A.; Bakker, H. J. *J. Chem. Phys.* **1999**, *111*, 1494–1500).

(61) This view is at odds with that of Giguere for HF [Giguere, P. A. *J. Chem. Educ.* **1979**, *56*, 571–575. Giguere, P. A. *Chem. Phys.* **1981**, *60*, 421–423], as is discussed in ref 39.

(59) Lias, S. G.; Bartmess, J. E.; Liebman, J. F.; Holmes, J. L.; Levin, R. D.; Mallard, W. G. *J. Phys. Chem. Ref. Data* **1988**, *17*, 1–861.

The relationship between the shift, $\Delta\omega$, in the hydrogen-bonded OH stretching frequency and the binding enthalpy, ΔH_{bind} (or energy), of the cluster is seen to be nonlinear in both models. This is in agreement with a combination of experimental data¹² and the calculations of Yates et al.¹⁷ The experimental data^{12,18,19} alone are suggestive of a nonlinear relationship. However, this probably will not be unambiguously established without measurements of the frequency shift in the $\text{F}^- \cdots \text{H}_2\text{O}$ cluster,¹⁵ whose importance we have argued for within.

By examining the Löwdin charges on different fragments within the cluster using ab initio calculations, the importance of charge-transfer effects is observed, particularly as the OH bond is stretched away from equilibrium. In addition, this allows the distinction to be made between polarization effects, in which charge is only rearranged within the water molecule, and charge transfer. A natural bond orbital analysis of the halide–water clusters supports a Mulliken picture of the hydrogen bonding.

The inclusion of a charge-transfer valence bond state allows us to estimate its contribution to the electronically adiabatic ground states of the clusters. We find that the importance of charge transfer decreases on moving down the group of halogens

(62) Note added in proof: According to the calculations of Majumdar et al. (Majumdar, D.; Kim, J.; Kim, K. S. *J. Chem. Phys.* **2000**, *112*, 101–105), published after submission of the present work, the charge transfer in the S_1 excited electronic state for the halide–water series increases in the direction I^- , Br^- , Cl^- , but then falls by more than an order of magnitude for F^- . It would be of interest in future work to examine this behavior in the context of the present type of analysis.

(63) Scheiner, S.; Cuma, M. *J. Am. Chem. Soc.* **1996**, *118*, 1511–1521.

($\text{F} > \text{Cl} > \text{Br} > \text{I}$). This is in strong contrast to the result one would predict by simply examining the electron affinities of the four halogens.^{59,62} However, the $\text{X}^- \cdots \text{O}$ distance is shorter the smaller the halide anion, and the shorter the distance the more facile is the charge transfer in the cluster.

Finally, we note that the charge-transfer effects should exhibit an isotope effect. That is, according to the present analysis, and in the simplest view, replacing the hydrogen-bonded H atom by deuterium will diminish the charge-transfer contributions to the O–D frequency shift. This is because, as seen in Figure 8, the charge-transfer character increases as the O–H bond is stretched, and the lower frequency of the O–D stretch would result in smaller classical vibrational turning points. Establishing whether such a simple view in fact holds requires attention to the isotope effect on all vibrations in the complex⁶³ and is a topic for future research.

Acknowledgment. This work was supported in part by the U.S. National Science Foundation through Grants CHE-9700419 and CHE-9709195. This work was completed while J.T.H. was a visiting Condorcet Chair of Chemistry at Ecole Normale Supérieure, Paris, Summer 1999, and he thanks the members of the Département de Chimie for their hospitality. We also thank Profs. Mark A. Johnson and Mitchio Okumura for useful discussions and Dr. Akihiro Morita for helpful comments.

JA993058Q